

1 **A carboxylated Zn-phthalocyanine inhibits the fibril formation of**
2 **Alzheimer's amyloid β peptide.**

3 Shatera Tabassum¹, Abdullah Md. Sheikh¹, Shozo Yano¹, Takahisa Ikeue²,
4 Makoto Handa², Atsushi Nagai^{1*}

5 ¹Department of Laboratory Medicine, Shimane University School of Medicine,
6 89-1 Enya Cho, Izumo 693-8501, Japan

7 ²Department of Material Science, Interdisciplinary Faculty of Science and
8 Engineering, Shimane University, 1060 Nishikawatsu, Matsue 690-8504, Japan

9

10 Running title: ZnPc inhibits A β fibril formation

11 *Address correspondence to:

12 Atsushi Nagai

13 Department of Laboratory Medicine

14 Shimane University School of Medicine

15 89-1 Enya Cho, Izumo 693-8501,

16 Japan

17 Tel.: +81-0853-20 2312

18 Fax: +81-0853-20 2312

19 E mail anagai@med.shimane-u.ac.jp

20 Key words: amyloid β , phthalocyanine, Alzheimer's disease, fibril formation, near
21 infrared.

22

1 **Abstract:**

2 Amyloid β (A β), a 39 to 42 amino acid long peptide derives from amyloid
3 precursor protein, is deposited as fibrils in Alzheimer's disease (AD) brains and
4 considered as main cause of the disease. We have investigated the effects of a
5 water-soluble Zn-phthalocyanine [ZnPc(COONa)₈], a macrocyclic compound
6 having near infrared optical property, on *in vitro* A β fibril formation process. The
7 ThT fluorescence assay demonstrated that ZnPc(COONa)₈ significantly inhibited
8 A β fibril formation, by increasing the lag time and dose-dependently decreasing
9 the fibril level at the plateau. Moreover, it increased the destabilization of the
10 preformed A β fibrils, and consequently increased the low molecular weight
11 species. Immunoprecipitation using A β -specific antibody followed by near
12 infrared scanning showed the binding of ZnPc(COONa)₈ to A β ₁₋₄₂. As a result,
13 the hydrophobicity of the A β ₁₋₄₂ fibril formation microenvironment was decreased.
14 CD spectroscopy revealed that α helix structure was increased and β sheet was
15 decreased when ZnPc(COONa)₈ was added to A β ₁₋₄₀ in fibril formation buffer.
16 Further, SDS-PAGE and dot blot immunoassay demonstrated that
17 ZnPc(COONa)₈ delayed the reduction of low molecular weight and appearance
18 of higher molecular weight oligomer species of A β ₁₋₄₂. The toxicity of

1 ZnPc(COONa)₈ on the culture of a neuronal cell line (A1) was evaluated by MTT
2 cell viability assay. The result showed that ZnPc(COONa)₈ did not decreased the
3 viability, rather protected A1 cells from Aβ₁₋₄₂-induced toxicity. Thus, our results
4 demonstrated that ZnPc(COONa)₈ was bound to Aβ and decreased the
5 hydrophobicity of fibril formation microenvironment. This change of
6 microenvironment consequently inhibited oligomer and fibril formation process.

1 **Introduction:**

2 Alzheimer's disease (AD) is a common dementia disease of the elderly
3 [1]. Pathologically, the disease is characterized by degeneration of neurons,
4 mainly cholinergic type, in the hippocampal and cortical areas [2,3]. Histological
5 examination demonstrates the presence of dystrophic neurons and reactive glial
6 cells in those areas; with extracellular deposition of amyloid β ($A\beta$) peptide and
7 intracellular formation of neurofibrillary tangles [2]. A large body of evidences
8 suggests that $A\beta$ peptide has a critical role in the pathogenesis of AD. For
9 example, the genetic conditions that affect the production or processing of $A\beta$
10 precursor protein and increase the peptide burden, is related to AD lesion
11 formation and progression of the disease [4- 10]. Such increased level causes
12 the peptide to aggregate to oligomers or polymeric fibrils and deposits in the
13 brain parenchyma [6]. In vitro cell culture system demonstrated that compared to
14 $A\beta$ monomers, the aggregated forms especially oligomers are more toxic to the
15 neurons [11, 12]; suggesting that $A\beta$ production as well as aggregation process
16 are vital for the disease pathogenesis. Hence, $A\beta$ peptide production as well as
17 aggregation process might be a good target for the diagnosis and the therapy of
18 AD.

19 Recently, immense progresses have been achieved in the research
20 regarding the pathophysiology of AD in the field of genetics and molecular
21 pathology. Bases on the findings of pathophysiological mechanisms of the
22 disease, molecules that have inhibitory effects on $A\beta$ peptide production and
23 peptide aggregation and enhance the fibril degradation process might be useful
24 for the therapy of the disease. Several compounds, reported to have

1 anti-amyloid activity on *in vitro* system and on animal models, are being tested in
2 the clinical trials [13, 14]. However, a disease modifying therapeutic system is
3 still elusive.

4 Not only in the field of therapy, the advancement in the field of diagnosis
5 is limited as well. Several groups are trying to use A β peptide in the CSF or
6 deposited in the brain parenchyma as a diagnostic marker [15, 16]. The
7 deposited A β can be visualized by PET imaging; however, the principal
8 shortcoming of this procedure is the requirement of a specialized technical setup
9 [16]. From a technical point of view, near infrared (NIR) is a suitable technique
10 for *in vivo* imaging. It has an optical imaging window from approximately 600 to
11 1000 nm, where the absorption coefficient of tissue is at a minimum and results
12 low background [17]. NIR has higher tissue penetration ability compared to
13 visible light [17]. Recently, it has been demonstrated that phthalocyanines, a NIR
14 fluorophore, interact with α -Synuclein and affect the fibril formation process
15 depending on the presence of metal at their central aromatic macrocyclic
16 structure [18]. Another report showed that iron containing phthalocyanine
17 interacts with toxic oligomeric state of A β ₁₋₄₀ and converts it to amyloid fibril
18 meshwork [19]. These findings are suggesting that phthalocyanines might be
19 useful as an amyloid fibril modifying agent in the therapy as well as
20 amyloid-specific probe in the NIR imaging to analyze the deposited A β peptide in
21 AD subjects.

22 Most of the phthalocyanine species are hydrophobic, and have a
23 tendency to aggregate in aqueous medium resulting a self-quenching effect on
24 their excited state [20, 21]. To circumvent that setback, we prepared a water

1 soluble Zn-containing phthalocyanine (ZnPc) by conjugating sodium carboxylate
2 group. To test whether it can be used as an amyloid fibril modifying agent or an
3 *in vivo* NIR probe, we investigated the detail interactions of carboxylated ZnPc
4 with A β peptide and their neurotoxic effects. We have found that carboxylated
5 ZnPc binds to A β peptide and inhibits peptide aggregation process.

6 **Result:**

7 **Interactions of Phthalocyanins with A β ₁₋₄₀ and A β ₁₋₄₂ during the process of**
8 **fibril formation.** To investigate the interactions, A β ₁₋₄₀ (50 μ M) or A β ₁₋₄₂ (12.5
9 μ M) was incubated with increasing concentrations of various types of
10 phthalocyanines (Pc) including ZnPc(COONa)₈, ZnPc(COONa)₁₆,
11 ZnPc(COOC₅H₁₁)₈ and PdPc dimers in a fibril forming buffer for 48 h or 24 h,
12 respectively. Evaluation of the fibril formation by ThT fluorescence assay at the
13 end of incubation revealed that ZnPc(COONa)₈ efficiently and dose dependently
14 inhibited the fibril formation of both A β ₁₋₄₀ and A β ₁₋₄₂ peptides (figure 1A and 1B).
15 The effects were more pronounced in the case of A β ₁₋₄₀ (compare figure 1A and
16 1B). ZnPc (COONa)₁₆ also demonstrated modest inhibitory effects on A β ₁₋₄₀ and
17 A β ₁₋₄₂ fibril formation at higher concentrations (figure 1C and 1D). PdPc dimer
18 inhibited fibril formation of A β ₁₋₄₀ only at higher concentrations (figure 1G and
19 1H). On the other hand, ZnPc(COOC₅H₁₁)₈ significantly and dose dependently

1 increased fibril formation of A β ₁₋₄₀ peptide, without showing such effects on
2 A β ₁₋₄₂ (figure 1E and 1F).

3 **Effects of ZnPc(COONa)₈ on the fibril formation kinetics of A β ₁₋₄₀ and A β ₁₋₄₂**

4 **peptides.** In order to investigate the fibril formation kinetics, A β ₁₋₄₀ (50 μ M) or
5 A β ₁₋₄₂ (12.5 μ M) was incubated in the absence or presence of 5 μ M
6 ZnPc(COONa)₈ and fibril formation was evaluated in a function of time. The
7 results demonstrated that both A β ₁₋₄₀ and A β ₁₋₄₂ fibril formation follow a typical
8 sigmoid kinetics with lag time of about 12 h and 8 h, respectively (figure 2 A and
9 2B). Then the fibril formation increased exponentially and reached plateaus at
10 48 h in the case of A β ₁₋₄₀, and 24 h in the case of A β ₁₋₄₂ (figure 2 A and 2B).

11 However, when incubated in the presence of ZnPc(COONa)₈, the lag time was
12 extended to 24 h and reached a plateau at 72 h in the case of A β ₁₋₄₀ (figure 2C).

13 In the case of A β ₁₋₄₂, addition of ZnPc(COONa)₈ increased the lag time to
14 between 8 and 16 h and reached a plateau at 16 h (figure 2D). Moreover,
15 ZnPc(COONa)₈ significantly decreased the fluorescence levels at the plateaus
16 of both A β ₁₋₄₀ (A β ₁₋₄₀=57 \pm 8.3 vs A β ₁₋₄₀+ZnPc(COONa)₈=12.3 \pm 2.4) and A β ₁₋₄₂
17 (A β ₁₋₄₂=20.1 \pm 0.8 vs A β ₁₋₄₂+ZnPc(COONa)₈=4.5 \pm 0.4).

18 Next, the fibril morphology was evaluated by transmission electron

1 microscopy. The results revealed that ZnPc(COONa)₈ did not change the overall
2 morphology of Aβ₁₋₄₀ or Aβ₁₋₄₂ (figure 2 E).

3 In this study, ThT fluorescence assay was mainly employed for the
4 quantitative analysis Aβ fibril. However, the presence of ZnPc(COONa)₈ could
5 affect ThT fluorescence [22] and the observed inhibitory effect might actually be
6 the consequence of that effect. To confirm the inhibitory effect, after fibril
7 formation of Aβ₁₋₄₂ (100 μM) in the absence or presence of ZnPc(COONa)₈ (5
8 μM) for 24 h, the fibrils were removed from the samples by filtration. As a result,
9 the filtrate contained only non-fibrillar Aβ₁₋₄₂, as revealed by ThT fluorescence
10 assay. Then protein concentration of the filtrate was measured. The result
11 showed that the protein level in the filtrate was 235 ± 8.2% higher in Aβ₁₋₄₂
12 sample containing ZnPc(COONa)₈, compared to Aβ₁₋₄₂ alone condition (figure
13 2F).

14 **Effects of ZnPc(COONa)₈ on the stability of Aβ fibrils.** Next, the effects of
15 ZnPc(COONa)₈ on the stability of Aβ fibrils was investigated. Increasing
16 concentrations of ZnPc(COONa)₈ was added to preformed fibrils of Aβ₁₋₄₀ and
17 Aβ₁₋₄₂, and incubated for 24 h. ThT fluorescence assay at the end of incubation
18 showed that ZnPc(COONa)₈ dose-dependently decreased both Aβ₁₋₄₀ and Aβ₁₋₄₂

1 fibril levels (figure 3A and 3B). Moreover, evaluation of the molecular species by
2 SDS PAGE confirmed that $\text{ZnPc}(\text{COONa})_8$ increased low molecular weight
3 species of $\text{A}\beta_{1-40}$ and $\text{A}\beta_{1-42}$, at least at high concentrations (figure 3C and 3D).

4 **Effects of Sodium Azide on $\text{A}\beta$ fibril formation.** Phthalocyanines are reported
5 to produce singlet oxygen [23] . We investigated whether singlet oxygen is
6 responsible for the inhibitory effects of $\text{ZnPc}(\text{COONa})_8$. To evaluate the possible
7 effects of singlet oxygen produced by $\text{ZnPc}(\text{COONa})_8$ on $\text{A}\beta$ fibril formation, we
8 used sodium azide (NaN_3) as a singlet oxygen scavenger [24]. First, the effect of
9 NaN_3 alone on $\text{A}\beta$ fibril formation was investigated. Increasing concentrations of
10 NaN_3 (up to 50 mM) did not alter $\text{A}\beta_{1-40}$ and $\text{A}\beta_{1-42}$ fibril formation (figure 4A and
11 4B). Next, increasing concentrations of NaN_3 (up to 50 mM) were incubated with
12 $\text{A}\beta_{1-40}$ and $\text{A}\beta_{1-42}$ in the presence of $\text{ZnPc}(\text{COONa})_8$. The ThT fluorescence
13 analysis demonstrated that NaN_3 had no effect on $\text{ZnPc}(\text{COONa})_8$ -mediated
14 inhibition of $\text{A}\beta_{1-40}$ and $\text{A}\beta_{1-42}$ fibril formation (figure 4C and 4D).

15 **Binding of $\text{ZnPc}(\text{COONa})_8$ to $\text{A}\beta_{1-42}$ peptide.** Next, we investigated whether
16 $\text{ZnPc}(\text{COONa})_8$ directly binds to $\text{A}\beta$ peptide. To investigate the binding,
17 increasing concentrations of $\text{ZnPc}(\text{COONa})_8$ were added to $\text{A}\beta_{1-42}$ monomers or
18 preformed fibrils and incubated for 24 h in a fibril forming environment. $\text{A}\beta_{1-42}$

1 was immunoprecipitated with A β specific antibody, and the level of
2 ZnPc(COONa)₈ in the immunoprecipitate was evaluated by near-infrared
3 scanning. The results demonstrated that in the case of A β ₁₋₄₂ monomer, near
4 infrared signal of ZnPc(COONa)₈ in the immunoprecipitates were increased
5 linearly with increasing dose of the compound (figure 5A). Similar effects was
6 observed in the case of preformed A β ₁₋₄₂ fibrils, however, the signal intensities
7 were much less compared to corresponding A β ₁₋₄₂ monomer conditions (figure
8 5A).

9 **Effects of ZnPc on the fibril formation micro-environment.** To explore the
10 mechanisms further, we investigated whether the binding of ZnPc(COONa)₈ has
11 any effect on the microenvironment of A β fibril formation. The hydrophobic
12 amino acids in A β peptide as well as hydrophobic microenvironment is shown to
13 play a vital role in the fibril formation process (25-27).

14 8-anilino-1-naphthalenesulfonic acid (ANS) is used as a hydrophobic fluorescent
15 probe. In aqueous solution the fluorescence of ANS is minimal. Upon binding to
16 nonpolar amino acids, ANS fluorescence increases and shows a blue shift.
17 Hence, ANS is used to analyze the conformational changes of proteins or
18 peptides in a solution [28]. Our ANS fluorescence results showed that incubation

1 of A β ₁₋₄₂ in fibril formation buffer for 4 h increased the fluorescence intensities
2 with a blue shift (figure 5B, 5C and 5D). But when ZnPc(COONa)₈ added to the
3 buffer, the intensities decreased significantly and the maxima showed a red shift
4 compared to their A β ₁₋₄₂-only counterpart (figure 5B, 5C and 5D).

5 **Effects of ZnPc(COONa)₈ on the secondary structures and the molecular**
6 **species of A β peptide.** Several reports have demonstrated that hydrophobic
7 interaction plays an important role in the secondary structures and the
8 aggregation of A β peptides [25, 29, 30]. As ZnPc(COONa)₈ decreased the
9 hydrophobicity of A β , we investigated whether it had any effect on the secondary
10 structure of the peptide. ZnPc(COONa)₈ (2 μ M) was added to A β ₁₋₄₀ (100 μ M)
11 monomers in a fibril forming buffer, and incubated at 37°C for 0 and 2 h. Then
12 the samples were diluted with water to make final concentrations of A β ₁₋₄₀ and
13 ZnPc(COONa)₈ to 10 μ M and 0.2 μ M, respectively. The results of CD
14 spectroscopy (figure 6A) showed that in fibril formation buffer, about 37.2 \pm 7.6%
15 of the peptide adopt β sheet structure, whereas only 5 \pm 2.3% was α helix. After 2
16 h incubation, although the percentage of α helix did not change much
17 (3.7 \pm 1.5%), the peptide adopting β sheet was increased to 48.6 \pm 0.2%. When
18 ZnPc(COONa)₈ was added to the fibril formation buffer, 18.7 \pm 0.9% peptide

1 adopted α helix structure, whereas β sheet was only $4.9 \pm 3\%$. After 2 h
2 incubation, the percentage of α helix and β sheet in this condition was 17.6 ± 3.5
3 and 17.2 ± 5.9 , respectively.

4 Next, after fibril formation in the absence or presence of $\text{ZnPc}(\text{COONa})_8$,
5 the peptide was separated by SDS-PAGE and $\text{A}\beta$ species were visualized by
6 Coomassie Blue. The results demonstrated that in our fibril formation system,
7 $\text{A}\beta_{1-42}$ existed mainly as monomer, dimer and trimer. Dimer and trimer were
8 started to decrease after 1 h incubation, and monomer was decreased from 2 h.
9 $\text{ZnPc}(\text{COONa})_8$ inhibited the time dependent reduction of the low molecular
10 weight $\text{A}\beta_{1-42}$ species, which was evident at least at 1, 2 and 4 h (figure 6B).

11 As low molecular weight $\text{A}\beta$ species aggregated to become higher
12 molecular weight oligomer and fibrils, the effects of $\text{ZnPc}(\text{COONa})_8$ on $\text{A}\beta_{1-42}$
13 oligomers were investigated. The dot blot immunoassay using an oligomer
14 specific antibody demonstrated that $\text{A}\beta_{1-42}$ oligomers were detectable after 4 h
15 incubation (figure 6C). $\text{ZnPc}(\text{COONa})_8$ delayed the appearance of $\text{A}\beta_{1-42}$
16 oligomers to 8 h (figure 6C).

17 **Effects of $\text{ZnPc}(\text{COONa})_8$ on $\text{A}\beta_{1-42}$ -induced cytotoxicity.** Oligomers of $\text{A}\beta$
18 peptides are considered to be more cytotoxic than the monomers [11, 12]. As

1 ZnPc(COONa)₈ inhibited oligomer formation, we explored whether it can affect
2 Aβ-induced cytotoxicity. The cytotoxic properties of Aβ₁₋₄₂ and ZnPc(COONa)₈
3 was analyzed using a neuronal cell line (A1) culture. Morphological study of A1
4 cell culture showed that increasing concentrations of Aβ₁₋₄₂ decreased the cell
5 density, and the cell body became round and smaller in size (figure 7A).
6 ZnPc(COONa)₈ alone did not alter the cell density or the morphology of the
7 cultured cells (figure 7A). Interestingly, addition of ZnPc(COONa)₈ in the culture
8 caused a partial rescue from Aβ₁₋₄₂-induced reduction of cell density and round
9 cell morphology (figure 7B).

10 To examine further the cytotoxic properties, cell viability was evaluated
11 by MTT assay. A1 cells were cultured in the presence of increasing
12 concentrations of Aβ₁₋₄₂ or ZnPc(COONa)₈ for 48 h, and MTT assay was done.
13 The results revealed that Aβ₁₋₄₂ dose-dependently decreased the viability of A1
14 cells, whereas ZnPc(COONa)₈ did not show such effects (figure 7C). Next, A1
15 cells were cultured with 5 μM Aβ₁₋₄₂ in the presence of increasing concentrations
16 of ZnPc(COONa)₈. The results demonstrated that ZnPc(COONa)₈ partially
17 rescued the cells from Aβ₁₋₄₂-induced cytotoxicity in a dose dependent manner
18 (figure 7D).

1 **Discussion:**

2 In this study, we have demonstrated that a water soluble
3 Zn-phthalocyanine [ZnPc(COONa)₈] has inhibitory effects on Alzheimer's A β
4 peptide aggregation process at *de novo* formation and dissociation and
5 re-association stage. As a possible mechanism, we have found that
6 ZnPc(COONa)₈ binds to the A β peptide and change the microenvironment of the
7 fibril formation process. A β aggregation and deposition play a vital role in AD
8 pathogenesis and could be used as a marker of the disease [2]. Due to its near
9 infrared optical property, the binding capacity and inhibition A β fibril formation,
10 ZnPc(COONa)₈ could be used for therapy as well as a diagnostic imaging probe
11 for AD.

12 The dose-dependent experiments showed that the inhibitory effects on
13 A β fibril formation are dependent on the species of phthalocyanines. In a report,
14 it has been shown that tetrasulfonated phthalocyanines interact with α -Synuclein
15 during the fibril formation process depending on the presence of metals at the
16 macrocyclic center [18]. Another study showed that iron containing
17 phthalocyanine convert A β ₁₋₄₀ oligomer to fibril meshwork [19]. Hence, it is
18 suggested that the interaction of phthalocyanines and A β is structure dependent.

1 ZnPc(COOC₅H₁₁)₈ and PdPc dimer were dissolved in chloroform, and sodium
2 carboxylated Pcs were in water, which raises the possibility that the differential
3 interaction is dependent on the hydrophilic properties of the compounds.
4 However, ZnPc(COONa)₈ showed much stronger inhibitory effects than
5 ZnPc(COONa)₁₆ despite of having similar solubility, suggesting that structural
6 differences of the compounds at least play a role in the process. Again,
7 ZnPc(COONa)₈ demonstrated much higher inhibitory effects on Aβ₁₋₄₀ than
8 Aβ₁₋₄₂ peptide fibril formation. Fibril formation of both Aβ₁₋₄₀ and Aβ₁₋₄₂ are
9 nucleation-dependent process, where the surfactant properties of the peptide
10 due to the presence of hydrophobic amino acids at the C-terminus play a pivotal
11 role [31]. The conformational difference due to the presence of two more
12 hydrophobic amino acids at the C-terminus causes Aβ₁₋₄₂ to polymerize much
13 faster than Aβ₁₋₄₀ does [32]. Such conformational difference of the peptides
14 might also responsible for the differential interaction of ZnPc(COONa)₈ with the
15 peptides.

16 ZnPc(COONa)₈ not only inhibited Aβ fibril formation process, but also
17 destabilize the pre-formed fibrils. Fibril formation is a dynamic process, where
18 association of the monomers to polymers, and dissociation of the polymers to

1 monomer and other low molecular weight species occur side by side. Initially, the
2 concentration of monomer and other low molecular weight species are high. As
3 a result, the rate of association is more than that of dissociation [33]. At the
4 plateau stage, the rate of association and dissociation reaches an equilibrium
5 state [33]. Our binding assay showed that $\text{ZnPc}(\text{COONa})_8$ had a higher binding
6 ability to monomers and other low molecular weight species than preformed
7 fibrils of $\text{A}\beta$ peptide. Therefore, in the destabilization experiment, the monomer
8 and the low molecular weight species of $\text{A}\beta$ might bound to $\text{ZnPc}(\text{COONa})_8$ after
9 dissociation from the fibrils. Such binding prevented them to recycle in the fibril
10 formation process. Indeed, we have found that addition of $\text{ZnPc}(\text{COONa})_8$ into
11 the fibrils increases the low molecular weight species, at least in the case of
12 $\text{A}\beta_{1-40}$.

13 Pthalocyanines are known to produce singlet oxygen in the presence of
14 light [23]. For that property, phthalocyanines are being used as photosensitizer in
15 the photodynamic therapy. Singlet oxygen is known to interact with the biological
16 molecules including proteins. Hence, as a possible mechanism of inhibition, the
17 role of singlet oxygen in the fibril formation process was investigated. Sodium
18 azide is known to scavenge singlet oxygen [24]. In our experiment, increasing

1 concentrations of sodium azide were used during the fibril formation, but even at
2 high concentration, sodium azide did not abolish the inhibitory effect. This result
3 is suggesting that the inhibitory effect is mediated through a singlet
4 oxygen-independent mechanism.

5 To investigate further about the mechanism, we found that ZnPc binds to
6 A β peptide during fibril formation process. Previous study showed that the
7 compounds having aromatic ring structure can interact with amyloid forming
8 peptides [34, 35]. For example, immunoglobulin light chain interacts with Congo
9 red, and this interaction actually inhibits the fibril formation [35]. Although we did
10 not examine which part of carboxylated ZnPc binds to the A β peptide, their
11 aromatic ring structure could be the possible the region. However, other species
12 of phthalocyanins including ZnPc(COOC₅H₁₁)₈ also contain aromatic rings.
13 Hence, if the aromatic rings are the only determinant for the binding and
14 subsequent interaction with A β , then the inhibitory effect would be more
15 generalized, not specific only for ZnPc(COONa)₈ and ZnPc(COONa)₁₆;
16 suggesting other parts of the compound, such as sodium carboxylated side
17 chains could also be important for the interaction. Several reports demonstrated
18 the interaction of Zn⁺ with A β peptide and subsequent modulation of fibril

1 formation (36, 37). The observation that mainly zinc containing phthalocyanines
2 interacted with A β peptide are suggesting that zinc might play an important role
3 in the interaction. Nevertheless, the differential effects of ZnPc(COONa)₈ and
4 ZnPc(COONa)₁₆ on A β fibril formation is suggesting that the structural difference
5 due to the presence of sodium carboxylate groups in the compound at least play
6 a role in the interaction with the peptide.

7 A β aggregation is a nucleation dependent process, where the
8 hydrophobic interaction of the peptide plays a vital role [29, 30]. The
9 microenvironment that exposes the C-terminal hydrophobic amino acids in an
10 aqueous environment is proposed to enhance the fibril formation process [29,
11 30]. ANS, a hydrophobic fluorescent dye, binds to exposed hydrophobic amino
12 acids of the proteins. It is minimally fluorescent in polar environment, which is
13 dramatically increased in nonpolar environment with a blue shift. Hence, this dye
14 is used to analyze the protein conformational changes [28]. We found that
15 addition of ZnPc(COONa)₈ caused a reduction of ANS fluorescence from an
16 early time point and maintained throughout our observation time., In previous
17 studies, ANS has been shown to bind to hydrophobic amino acid patches in A β
18 peptide. Due to the structural differences, each of the molecular species, such

1 as oligomers, prefibrillar aggregates and the mature fibrils might have different
2 binding affinity to ANS. Hence, the change in the ANS fluorescence might
3 suggest the changes in the proportion of the different molecular species of A β
4 caused by the binding of ZnPc(COONa)₈. Alternatively, a constant reduction of
5 ANS fluorescence from early time point could suggest a less hydrophobic
6 peptide micro-environment provided by ZnPc(COONa)₈. The β -sheet population
7 of the peptide, which is shown to be affected by hydrophobic environment [25],
8 was observed to be decreased by ZnPc(COONa)₈ from early time point of fibril
9 formation. Again, in our fibril formation condition, monomer, dimer, trimer and
10 tetramer were visible from the beginning of the experiments. With function of
11 time, those low molecular weight species decreased, and subsequently the
12 oligomers were increased. When ZnPc(COONa)₈ was added, the reduction of
13 such low molecular weight species and the appearance of oligomers was
14 delayed. Taken together, our results are suggesting that by decreasing the
15 hydrophobic microenvironment, ZnPc(COONa)₈ inhibits the nucleation and
16 oligomerization process.

17 Finally, the effects of ZnPc on the neuronal viability were investigated. As
18 shown in previous studies [38], our preliminary experiments demonstrated that

1 ZnPc(COONa)₈ could be accumulated inside the cells in a neuronal cell culture
2 system (data not shown). Hence, it is possible that internalized ZnPc(COONa)₈
3 affects the intracellular biological functions and alter the viability. As shown in the
4 results, ZnPc(COONa)₈ did not decrease the viability, rather it provided at least
5 some protection against Aβ-induced neuronal toxicity. Aβ oligomers are
6 considered to be the most toxic species of Aβ [11, 12]. By decreasing the
7 oligomer formation, ZnPc(COONa)₈ might confer such protection against the
8 Aβ-induced neurotoxicity.

9 Thus, our results demonstrated that water soluble ZnPc(COONa)₈ binds
10 to Aβ peptide and inhibits its oligomer and subsequent fibril formation process.
11 For its near infrared optical properties, Aβ binding, inhibitory and destabilizing
12 effects on fibril formation process, and neuroprotective properties against Aβ
13 peptide, it could be used as a safe diagnostic probe as well as a therapeutic tool
14 for AD.

15 **Materials and Methods**

16 **Materials**

17 The Aβ peptides Aβ₁₋₄₀ and Aβ₁₋₄₂ (Peptide Institute, Osaka, Japan)
18 were each dissolved in 0.1% NH₃ at a concentration of 250 μM, aliquoted
19 immediately (in order to avoid the need for repeated freeze-thaw cycles), and

1 stored at -70°C , according to the manufacturer's instructions. Chromatographic
2 data provided by the manufacturer confirmed the monomeric purity of the
3 peptides. Thioflavin T (ThT) was purchased from Wako Pure Chemicals
4 (Richmond, VA, USA), and deionized and filter sterile water was purchased from
5 Sigma-Aldrich (St Louis, MO, USA). Prestained protein size marker was
6 purchased from NIPPON Genetics EUROPE GmbH (Duren, Germany) and
7 4-20% Tris-glycine polyacrylamide from Bio-Rad (Hercules, CA, USA).
8 Nitrocellulose membrane for dot blot assay was obtained from Millipore (Billerica,
9 MA).

10 **Phthalocyanins**

11 In this study 4 types of phthalocyanins were used. The molecular
12 structures are shown in the supplemental figure 1. $\text{ZnPc}(\text{COONa})_8$ and
13 $\text{ZnPc}(\text{COONa})_{16}$ were dissolved in H_2O . $\text{ZnPc}(\text{COOC}_5\text{H}_{11})_8$ and PdPc dimer
14 were dissolved in chloroform. The phthalocyanines were dissolved at 1 mM
15 concentrations and stored at -20°C until use. The detail methods of preparation
16 of the phthalocyanines [39, 40] are described in the supplemental methods.

17 **A β peptide fibril formation**

18 For fibril formation, synthetic A β peptides were added to a fibril formation

1 buffer containing 50 mM phosphate buffer (pH 7.5) and 100 mM NaCl [41], with
2 desired concentrations of phthalocyanines. As a control, peptides were added to
3 a fibril formation buffer where phthalocyanines were replaced by their solvents.
4 The reaction mixtures were incubated at 37°C without agitation for the indicated
5 times, and then the fibril formation reaction was terminated by quickly freezing
6 the samples.

7 **Assessment of A β fibril formation**

8 The presence of β -sheet structures and the kinetics of fibril formation
9 were monitored by means of ThT fluorescence spectroscopy [41]. Samples were
10 diluted tenfold with glycine (pH 8.5, 50 mM final concentration) and ThT (5 μ M
11 final concentration). ThT fluorescence was measured using a fluorescence
12 spectrophotometer (F2500 spectrofluorimeter, Hitachi, Tokyo, Japan), with
13 excitation and emission wavelengths of 446 and 490 nm, respectively. The
14 normalized fluorescence intensity of A β peptides in the form of fibrils were
15 obtained by subtracting the fluorescence intensity of buffer alone from that of the
16 samples.

17 To assess further about the fibril formation, 25 μ g A β ₁₋₄₂ at 100 μ M
18 concentration in the absence or presence of ZnPc(COONa)₈ (5 μ M) were used

1 for fibril formation for 24 h. Then the fibrils were removed from the samples using
2 a 100 KDa cut off filter (amicom), and the filtrates were concentrated by
3 evaporation. The total protein in the filtrates was measured using a UV/Vis
4 spectrophotometer at 280 nm.

5 **Electron microscopy**

6 Electron microscopy was performed as described previously [41]. In brief,
7 after formation of A β (50 μ M) fibril in the absence or presence of ZnPc(COONa)₈
8 (5 μ M), 5 μ l of sample was applied to a carbon-coated Formvar grid (Nisshin EM,
9 Tokyo, Japan) and incubated for 1 min. The droplet was then displaced with an
10 equal volume of 0.5% v/v glutaraldehyde solution and incubated for an
11 additional 1 min. The grid was washed with a few drops of water and dried.
12 Finally, the peptide was stained with 10 μ l of 2% w/v uranyl acetate solution for 2
13 min. This solution was soaked off, and the grid was air-dried and examined
14 under an electron microscope (EM-002B, Topcon, Tokyo, Japan).

15 **ANS fluorescence spectroscopy**

16 The fluorescence intensity change of 8-anilino-1-naphthalene sulfonic
17 acid (ANS) was used to evaluate the relative exposure levels of hydrophobic
18 surfaces of A β ₁₋₄₂ aggregates. Fluorescence intensity measurements were

1 obtained using a Hitachi F2500 spectrofluorimeter, with excitation at 360 nm.
2 The emission spectra were read from 380 to 600 nm, at a scan rate of 300
3 nm/min. Slit widths for excitation and emission were 5 nm. The data of emission
4 maximum is presented as the mean \pm SEM of three independent experiments,
5 and is expressed in arbitrary fluorescence units.

6 **Gel electrophoresis and staining**

7 SDS PAGE was performed using a 4–20% gradient tris-glycine gel
8 system (Biorad). At the end of incubation, 2 μ g of A β peptide was mixed with 2x
9 SDS non-reducing sample buffer (Invitrogen, Carlsbad, CA, USA) making a total
10 volume of 20 μ l, incubated at 85°C for 2 min, and separated by electrophoresis.
11 The gel was washed briefly with water, fixed in fixation buffer (40% methanol
12 and 10% acetic acid) for 30 min, and stained with Coomassie Blue G250
13 (Biosafe Coomassie; Bio-Rad) for 1 h. The stained gel was washed with water
14 overnight and scanned using a gel scanner (Bio-Rad).

15 **Dot-blot immunoassay**

16 After fibril formation, 2 μ g of A β ₁₋₄₂ peptide was applied to a nitrocellulose
17 membrane using a manifold. Then the membrane was immunoblotted with an
18 oligomer-specific antibody (A11, Invitrogen). This oligomer-specific antibody

1 reacts specifically to a variety of soluble oligomeric protein/peptide aggregates
2 regardless of their amino acid sequence, and does not react with either
3 monomer species or insoluble fibrils [42]. It reacts only with A β oligomer species
4 of at least octamer. Immunoreactive oligomer was detected using infrared
5 dye-conjugated anti-rabbit IgG and Odessey infrared dye scanning system
6 (Li-Cor, Lincoln, NE, USA), according to the manufacturer's instructions.

7 **Phthalocyanine binding assay**

8 To determine the binding of ZnPc(COONa)₈ with A β peptide, A β ₁₋₄₂ (50
9 μ M) and indicated concentrations of ZnPc(COONa)₈ was incubated in a fibril
10 formation buffer for 24 h. To evaluate the binding with the fibrils, A β fibrils were
11 prepared by incubation of the peptide in a fibril formation buffer for 24 h. Then
12 indicated concentrations of ZnPc(COONa)₈ was added to the fibril to make the
13 concentration of the peptide 50 μ M, and further incubated for 24 h. Five
14 micrograms of peptide were immunoprecipitated with a monoclonal anti-A β
15 specific antibody (Santa Cruz, Dallas, Tx, USA). Then the immunoprecipitates
16 were taken in a ELISA plate and scanned at 680 nm wave length using Odessey
17 infrared scanner (Li-Cor) to detect ZnPc(COONa)₈ in the immunoprecipitate. As
18 a negative controls, fibril formation buffer containing indicated concentrations of

1 ZnPc(COONa)₈ was immunoprecipitated with anti-A β specific antibody, and
2 mouse normal IgG was used instead of anti-A β specific antibody to
3 immunoprecipitate A β plus ZnPc(COONa)₈ samples

4 **Analysis of the secondary structures of A β peptide**

5 To prepare the samples for the evaluation of secondary structures
6 during fibril formation process, ZnPc(COONa)₈ (2 μ M) was added to A β ₁₋₄₀ (100
7 μ M) monomers in a fibril forming buffer, and incubated at 37°C for 0 and 2 h.
8 Then the samples were diluted with water to make final concentrations of A β ₁₋₄₀
9 and ZnPc(COONa)₈ to 10 μ M and 0.2 μ M, respectively. Then the circular
10 dichroism (CD) spectral scan in the range of 190 – 250 nm was acquired at 50
11 nm/min speed using a Jasco J-720 spectropolarimeter (Jasco Corporation,
12 Tokyo, Japan) and a quartz cell with 3 mm optical path length. The results were
13 expressed as mean residue molar ellipticity, and the percentage of the
14 secondary structures in the samples were estimated by Protein Secondary
15 Structure Estimation Program (Jasco Corp.) using published reference CD
16 spectra [43].

17 **Cell culture**

18 A human neuronal cell line (A1) was generated by somatic fusion
19 between a human fetal cerebral neuron and a human neuroblastoma cell, which
20 showed morphological, electrophysiological and expressional features of
21 neurons [44]. A1 cells were cultured in 5% FBS (Gibco) containing DMEM

1 medium (Wako). During stimulation with $A\beta_{1-42}$ and $ZnPc(COONa)_8$, the
2 concentration of FBS was reduced to 1%. The photomicrographs of the cultured
3 cells were obtained with an inverted cell culture microscope equipped with a
4 digital photograph acquiring system.

5 **MTT cell viability assay**

6 The effects of $ZnPc(COONa)_8$ on $A\beta$ -induced neuronal toxicity was
7 evaluated by MTT cell viability assay, as described previously [45]. Briefly, A1
8 cells (3×10^3 /well) were seeded on the wells of a 96-well cell culture plate and
9 cultured for 48 h. The cells were treated with indicated concentrations of
10 $ZnPc(COONa)_8$, $A\beta_{1-42}$ or combined $A\beta_{1-42}$ and $ZnPc(COONa)_8$ in 100 μ l of 1%
11 FBS containing DMEM for 48 h. After incubation, 20 μ l of MTT solution (5 mg/ml)
12 was added to the culture medium and incubated for 3.5 h at 37°C. Then the
13 medium was removed carefully, MTT solvent (4 mM HCl, 0.1% Nondet P-40 in
14 isopropanol) was added and further incubated for 15 min at room temperature
15 after protecting from light. Then the absorbance was read at 590 nm. The
16 absorbance of the cells of normal culture condition was used as a control.

17 **Statistical analysis**

18 The results are expressed as mean \pm SEM of at least three independent

1 experiments. Statistical analysis for comparing mean values was performed
2 using one-way ANOVA, followed by Scheffe's post hoc test, or *student's t* test.
3 The fibril formation kinetics were analyzed using SigmaPlot software (Systat
4 Software Inc, San Jose, CA, USA). *p* values < 0.05 indicate statistical
5 significance.

6 **Acknowledgement:** This study is supported by JSPS KAKENHI Grant Number
7 24310102.

8 **Authors contributions.** ST planned and performed the experiments, analyzed
9 the data and prepared the manuscript. AS planned the experiments, analyzed
10 the data and prepared the manuscript. SY analyzed the data and prepared the
11 manuscript. MH prepared phthalocyanines, analyzed the data and prepared the
12 manuscript. TI prepared phthalocyanines, analyzed the data and prepared the
13 manuscript. AN planned the experiments, provided the reagents and other
14 essential materials, prepared the manuscript, and overall supervised the study.

15 **References:**

- 16 1. Rowland LP, Pedley TA & Merritt HH (2010) *Merritt's Neurology*, 12 edn. pp.
17 713- 717. Lippincott Williams & Wilkins. Philadelphia, PA
18 2. Duyckaerts C, Delatour B, & Potier MC (2009) Classification and basic
19 pathology of Alzheimer disease. *Acta Neuropathol* **118**, 5-36.

- 1 3. Francis PT, Palmer AM, Snape M & Wilcock GK (1999) The cholinergic
2 hypothesis of Alzheimer's disease: a review of progress. *J Neurol Neurosurg*
3 *Psychiatry* **66**, 137– 147
- 4 4. Champion D, Flaman JM, Brice A, Hannequin D, Dubois B, Martin C, Moreau V,
5 Charbonnier F, Didierjean O, Tardieu S & et al. (1995) Mutations of the presenilin
6 I gene in families with early-onset Alzheimer's disease. *Hum Mol Genet* **4**,
7 2373-2377.
- 8 5. Goate A, Chartier-Harlin MC, Mullan M, Brown J, Crawford F, Fidani L, Giuffra
9 L, Haynes A, Irving N, James L & et al. (1991) Segregation of a missense
10 mutation in the amyloid precursor protein gene with familial Alzheimer's disease.
11 *Nature* **349**, 704-706.
- 12 6. Hardy J & Selkoe DJ (2002) The amyloid hypothesis of Alzheimer's disease:
13 progress and problems on the road to therapeutics. *Science* **297**, 353-356.
- 14 7. Richards SJ, Waters JJ, Beyreuther K, Masters CL, Wischik CM, Sparkman
15 DR, White CL 3rd, Abraham CR & Dunnett SB (1991) Transplants of mouse
16 trisomy 16 hippocampus provide a model of Alzheimer's disease neuropathology.
17 *EMBO J* **10**, 297-303.
- 18 8. Sisodia SS, Kim SH & Thinakaran G (1999) Function and dysfunction of the
19 presenilins. *Am J Hum Genet* **65**, 7-12.
- 20 9. Xia W, Zhang J, Kholodenko D, Citron M, Podlisny MB, Teplow DB, Haass C,
21 Seubert P, Koo EH & Selkoe DJ (1997) Enhanced production and
22 oligomerization of the 42-residue amyloid beta-protein by Chinese hamster
23 ovary cells stably expressing mutant presenilins. *J Biol Chem* **272**, 7977-7982.
- 24 10. Yoshioka K, Miki T, Katsuya T, Ogihara T & Sakaki Y (1991) The 717Val----Ile

- 1 substitution in amyloid precursor protein is associated with familial Alzheimer's
2 disease regardless of ethnic groups. *Biochem Biophys Res Commun* **178**,
3 1141-1146.
- 4 11. Cotman CW, Whittemore ER, Watt JA, Anderson AJ & Loo DT (1994)
5 Possible role of apoptosis in Alzheimer's disease. *Ann N Y Acad Sci* **747**, 36-49.
- 6 12. Malaplate-Armand C, Florent-Bécharard S, Youssef I, Koziel V, Sponne I,
7 Kriem B, Leininger-Muller B, Olivier JL, Oster T & Pillot T (2006) Soluble
8 oligomers of amyloid-beta peptide induce neuronal apoptosis by activating a
9 cPLA2-dependent sphingomyelinase-ceramide pathway. *Neurobiol Dis* **23**,
10 178-189.
- 11 13. Iqbal K, Liu F. & Gong CX (2014) Alzheimer disease therapeutics: Focus on
12 the disease and not just plaques and tangles. *Biochem Pharmacol* **88**, 631-639.
- 13 14. Leger GC & Massoud F (2013) Novel disease-modifying therapeutics for the
14 treatment of Alzheimer's disease. *Expert Rev Clin Pharmacol* **6**, 423-442.
- 15 15. Cruchaga C, Ebbert MT & Kauwe JS (2014) Genetic discoveries in AD using
16 CSF amyloid and tau. *Curr Genet Med Rep* **2**, 23-29.
- 17 16. Petrella JR (2013) Neuroimaging and the search for a cure for Alzheimer
18 disease. *Radiology* **269**, 671-691.
- 19 17. Hilderbrand SA & Weissleder R (2010) Near-infrared fluorescence:
20 application to in vivo molecular imaging. *Curr Opin Chem Biol* **14**, 71-79.
- 21 18. Lee EN, Cho HJ, Lee CH, Lee D, Chung KC & Paik SR (2004)
22 Phthalocyanine tetrasulfonates affect the amyloid formation and cytotoxicity of
23 alpha-synuclein. *Biochemistry* **43**, 3704-3715.
- 24 19. Park JW, Ahn JS, Lee JH, Bhak G, Jung S & Paik SR (2008) Amyloid fibrillar

1 meshwork formation of iron-induced oligomeric species of Abeta40 with
2 phthalocyanine tetrasulfonate and its toxic consequences. *Chembiochem* **9**,
3 2602-2605.

4 20. Simon J & Vacus J (1995) Luminescence and anti-aggregative properties of
5 polyoxyethylene-substituted phthalocyanine complexes. *Adv Mater* **7**, 797-800.

6 21. Spikes JD (1986) Phthalocyanines as photosensitizers in biological systems
7 and for the photodynamic therapy of tumors. *Photochem Photobiol* **43**, 691-699.

8 22. Moss MA, Varvel NH, Nichols MR, Reed DK & Rosenberry T L (2004)
9 Nordihydroguaiaretic acid does not disaggregate beta-amyloid(1-40) protofibrils
10 but does inhibit growth arising from direct protofibril association. *Mol Pharmacol*
11 **66**, 592-600.

12 23. Agarwal R, Athar M, Urban SA, Bickers DR & Mukhtar H (1991) Involvement
13 of singlet oxygen in chloroaluminum phthalocyanine tetrasulfonate-mediated
14 photoenhancement of lipid peroxidation in rat epidermal microsomes. *Cancer*
15 *Lett* **56**, 125-129.

16 24. Bancirova M (2011) Sodium azide as a specific quencher of singlet oxygen
17 during chemiluminescent detection by luminol and Cypridina luciferin analogues.
18 *Luminescence* **26**, 685-688.

19 25. Kowalewski T & Holtzman DM (1999) In situ atomic force microscopy study
20 of Alzheimer's beta-amyloid peptide on different substrates: new insights into
21 mechanism of beta-sheet formation. *Proc Natl Acad Sci U S A* **96**, 3688-3693.

22 26. Marshall KE, Morris KL, Charlton D, O'Reilly N, Lewis L, Walden H & Serpell
23 LC (2011) Hydrophobic, aromatic, and electrostatic interactions play a central
24 role in amyloid fibril formation and stability. *Biochemistry* **50**, 2061-2071

- 1 27. Tjernberg LO, Callaway DJ, Tjernberg A, Hahne S, Lilliehöök C, Terenius L,
2 Thyberg J & Nordstedt C (1999) A molecular model of Alzheimer amyloid
3 beta-peptide fibril formation. *J Biol Chem* **274**, 12619-12625
- 4 28. Hawe A, Sutter M & Jiskoot W (2008) Extrinsic fluorescent dyes as tools for
5 protein characterization. *Pharm Res* **25**, 1487-1499.
- 6 29. Hills RD Jr & Brooks CL 3rd (2007) Hydrophobic cooperativity as a
7 mechanism for amyloid nucleation. *J Mol Biol* **368**, 894-901.
- 8 30. Serpell LC (2000) Alzheimer's amyloid fibrils: structure and assembly.
9 *Biochim Biophys Acta* **1502**, 16-30
- 10 31. Soreghan B, Kosmoski J & Glabe C (1994) Surfactant properties of
11 Alzheimer's A beta peptides and the mechanism of amyloid aggregation. *J Biol*
12 *Chem* **269**, 28551-28554.
- 13 32. El-Agnaf OM, Mahil DS, Patel BP & Austen BM (2000) Oligomerization and
14 toxicity of beta-amyloid-42 implicated in Alzheimer's disease. *Biochem Biophys*
15 *Res Commun* **273**, 1003-1007.
- 16 33. Morris AM, Watzky MA & Finke RG (2009) Protein aggregation kinetics,
17 mechanism, and curve-fitting: a review of the literature. *Biochim Biophys Acta*
18 **1794**, 375-97.
- 19 34. Porat Y, Abramowitz A & Gazit E (2006) Inhibition of amyloid fibril formation
20 by polyphenols: structural similarity and aromatic interactions as a common
21 inhibition mechanism. *Chem Biology Drug Des* **67**, 27-37.
- 22 35. McLaughlin RW, De Stigter JK, Sikkink LA, Baden EM & Ramirez-Alvarado
23 M (2006) The effects of sodium sulfate, glycosaminoglycans, and Congo red on
24 the structure, stability, and amyloid formation of an immunoglobulin light-chain

1 protein. *Protein Sci* **15**, 1710-22.

2 36. Bush AI, Pettingell WH, Multhaup G, d Paradis M, Vonsattel JP, Gusella JF,
3 Beyreuther K, Masters CL & Tanzi RE (1994) Rapid induction of Alzheimer A
4 beta amyloid formation by zinc. *Science* **265**, 1464-1467.

5 37. Esler WP, Stimson ER, Jennings JM, Ghilardi JR, Mantyh PW & Maggio JE
6 (1996) Zinc-induced aggregation of human and rat beta-amyloid peptides in vitro.
7 *J Neurochem* **66**, 723-732.

8 38. Trivedi NS, Wang HW, Nieminen AL, Oleinick NL & Izatt JA (2000)
9 Quantitative analysis of Pc 4 localization in mouse lymphoma (LY-R) cells via
10 double-label confocal fluorescence microscopy. *Photochem Photobiol* **71**, 634-9.

11 39. Ikeue T, Sonoda M, Kurahashi S, Tachibana H, Teraoka D, Sugimori T,
12 Kasuga K & Handa M (2010) Annulated dinuclear palladium (II) phthalocyanine
13 complex as an effective photo-oxidation catalyst for near-infrared region light.
14 *Inorganic Chemistry Comm.* **13**, 1170-1172.

15 40. Liu W, Jensen TJ, Fronczek FR, Hammer RP, Smith KM & Vicente MG
16 (2005) Synthesis and cellular studies of nonaggregated water-soluble
17 phthalocyanines. *J Med Chem* **48**, 1033-1041.

18 41. Sheikh AM & Nagai A (2011) Lysophosphatidylcholine modulates fibril
19 formation of amyloid beta peptide. *FEBS J* **278**, 634-642.

20 42. Kaye R, Head E, Thompson JL, McIntire TM, Milton SC, Cotman CW &
21 Glabe CG (2003) Common structure of soluble amyloid oligomers implies
22 common mechanism of pathogenesis. *Science* **300**, 486-489.

23 43. Yang JT, Wu CS, Martinez HM (1986) Calculation of protein conformation
24 from circular dichroism. *Methods Enzymol* **130**, 208-269

1 44. Nagai A, Suzuki Y, Baek SY, Lee KS, Lee MC, McLarnon JG & Kim SU
2 (2002) Generation and characterization of human hybrid neurons produced
3 between embryonic CNS neurons and neuroblastoma cells. *Neurobiol Dis* **11**,
4 184-198.

5 45. Nagai A, Ryu JK, Terashima M, Tanigawa Y, Wakabayashi K, McLarnon JG,
6 Kobayashi S, Masuda J & Kim SU 2005. Neuronal cell death induced by cystatin
7 C in vivo and in cultured human CNS neurons is inhibited with cathepsin B. *Brain*
8 *Res* **1066**, 120-128.

9

10 **Supplementary Materials and Methods**

11 **Synthesis of Phthalocyanines**

12 Molecular structures of phthalocyanines are shown in the supplemental
13 figure 1. They were prepared by following the procedures described in previous
14 reports (supplemental references 1 and 3).

15 **ZnPc(COOC₅H₁₁)₈ :**

16 The reaction between 4,5-dichlorophthalonitrile (1.0 g, 5.1 mmol) and
17 *n*-hexyl-4-hydroxybenzoate (4.3 g, 19.3 mmol) was done in DMF (60 ml) by
18 stirring in the presence of K₂CO₃ (4 × 4 g) at 65 °C for 24 h. The reaction mixture
19 was poured into ice-cold water to give a white-brown precipitate, which was
20 extracted with CHCl₃ (5 × 100 ml). The organic extracts were dried over
21 anhydrous MgSO₄ (25 g) and concentrated under vacuum to give a yellow oil.
22 Recrystallization from methanol gave
23 4,5-bis[(4-hexyloxy carbonyl)phenoxy]phthalonitrile as a white solid (yield: 2.2 g).
24 The obtained compound (460 mg, 0.81 mmol) was employed for the reaction

1 with Zn(OAc)₂•2H₂O (65 mg, 0.30 mmol)) in *n*-pentanol (10 ml) containing a few
2 drops of 1,8-diazabicyclo[5.4.0]undec-7-ene (DBU). After the reaction mixture
3 was refluxed overnight, the volatiles were removed under a reduced pressure
4 condition to give a greenish blue solid. Recrystallization of the crude product
5 from EtOH/H₂O gave a green solid. In the nitrile cyclization reaction in
6 *n*-pentanol, hexyloxy groups on the nitrile were replaced by pentoxy groups
7 coming from the reaction solvent. Hence, the obtained green solid was the title
8 complex ZnPc(COOC₅H₁₁)₈ (yield: 280 mg).

9 **ZnPc(COONa)₁₆:**

10 4,5-Dichlorophthalonitrile, 5-hydroxyisophthalate, and K₂CO₃ were
11 mixed in DMF and stirred at 65 °C for 24 h. The reaction mixture was poured into
12 ice-cold water to give a white-brown precipitate, which was extracted with CHCl₃.
13 The organic extracts were dried over anhydrous MgSO₄ and concentrated under
14 vacuum to give a yellow oil. After recrystallization from methanol,
15 4,5-bis[(3,5-bismethoxycarbonyl)phenoxy]phthalonitrile (1st compound) was
16 obtained as a white solid.

17 The 1st compound was mixed with Zn(OAc)₂•2H₂O and a few drops of
18 1,8-diazabicyclo[5.4.0]undec-7-ene (DBU) in *n*-pentanol and refluxed overnight.
19 The volatiles were removed under vacuum to give a greenish blue solid, which
20 was purified by column chromatography using dichloromethane/ethyl acetate
21 (20:1) for elution. The crude product was recrystallized from THF/MeOH to give
22 the 2nd compound zinc(II)
23 2,3,9,10,16,17,23,24-octakis[(3',5'-bispentyloxycarbonyl)phenoxy]phthalocyanin
24 e as a green solid.

1 The 2nd compound was dissolved in THF and added slowly to a
2 saturated NaOH solution in water/methanol (1:5) (100 ml). The mixture was
3 stirred at 40°C for 4 h, and the resulting precipitate was filtered and washed
4 repeatedly with MeOH and CHCl₃. The crude product was dissolved in water
5 and neutralized using 1M HCl until pH 7. The title compound ZnPc(COONa)₁₆
6 was precipitated upon addition of ethanol to yield a green solid .

7 **ZnPc(COONa)₈ :**

8 A saturated NaOH solution in water/methanol (1:5) (100 ml) was added
9 slowly to a THF (5 ml) of ZnPc(COOC₆H₁₃)₈ (200 mg). The mixture was stirred at
10 40°C for 4 h, and the resulting precipitate was filtered and washed repeatedly
11 with MeOH and CHCl₃. The crude product was dissolved in water and
12 neutralized using 1M HCl until pH 7. Then ethanol was added to give the
13 precipitation of ZnPc(COONa)₈, which was obtained as a green solid (yield: 66
14 mg).

15 **PdPc Dimer:**

16 4,5-Bis(2,6-dimethylphenoxy)phthalonitrile (997 mg, 2.7 mmol),
17 bis(1,3-diiminoisoindoline) (115 mg, 0.54 mmol), and PdCl₂ (295 mg, 1.7 mmol)
18 were mixed and heated in the presences of *n*-propanol (10 ml) and
19 1,8-diazabicyclo[5.4.0]undec-7-ene (DBU) (1.0 ml) at 110°C for 30 h. After the
20 reaction mixture was cooled, toluene (30 ml) was added into the mixture and the
21 precipitate was filtered, and vacuum-dried to give a green solid. Then, the green
22 solid was dissolved in toluene and separated by GPC chromatography using
23 toluene as an eluent, and obtained two major fractions. The title PdPc dimer was
24 obtained from the first fraction (yield: 112 mg) and the mononuclear PcPc was

1 from the second fraction (yield: 645 mg).

2

3 Supplemental references

4 1. Liu, W., Jensen, T. J., Fronczek, F. R., Hammer, R. P., Smith, K. M. & Vicente,

5 M. G. (2005) Synthesis and cellular studies of nonaggregated water-soluble

6 phthalocyanines, *Journal of medicinal chemistry*. 48, 1033-41.

7 2. Ikeue, T., Sonoda, M., Kurahashi, S., Tachibana, H., Teraoka, D., Sugimori, T.,

8 Kasuga, K. & Handa, M. (2010) Annulated dinuclear palladium (II)

9 phthalocyanine complex as an effective photo-oxidation catalyst for

10 near-infrared region light, *Inorganic Chemistry Comm.* 13, 1170-1172.

11 3. Verdree, V. T., Pakhomov, S., Su G., Allen, M. W., Countryman, A. C.,

12 Hammer, R. O., Soper S. A. (2007) Water Soluble Metallo-Phthalocyanines: The

13 Role of Functional Groups on the Spectral and Photophysical Properties, *J.*

14 *Fluoresc.* 17, 547-563.

15

16 **Supplementary figure legend**

17 **Supplementary Figure 1:** Structures of phthalocyanines used in the

18 experiments. The chemical structure of $\text{ZnPc}(\text{COONa})_8$ (A), $\text{ZnPc}(\text{COONa})_{16}$ (B),

19 $\text{ZnPc}(\text{OOC}_5\text{H}_{11})_8$ (C) and Pd-Pc dimer (D) are shown.

20 **Figure legends**

21 **Figure 1: Effect of Phthalocyanines on A β peptide fibril formation.** A β_{1-40}

22 (50 μM) (A, C, E and G) or A β_{1-42} (12.5 μM) (B, D, F and H) peptides were

1 incubated in a fibril forming buffer for 48 h and 24 h, respectively, in the presence
2 of indicated concentrations of ZnPc(COONa)₈ (A and B), ZnPc(COONa)₁₆ (C
3 and D), ZnPc(COOC₅H₁₁)₈ (E and F) and PdPc dimer (G and H). Total fibril
4 formed at the end of incubation was evaluated by ThT fluorescence assay, as
5 described in the Materials and Methods. Data shown here are the averages ±
6 SEM of at least 3 independent experiments, and presented as percent of Aβ
7 peptide alone (control) condition. *p<0.05, ‡p<0.01 and †p<0.001 vs
8 corresponding 0.1 μM condition

9 **Figure 2: Effects of ZnPc(COONa)₈ on the fibril formation kinetics of Aβ**

10 **peptides.** Aβ₁₋₄₀ (50 μM) (A and C) or Aβ₁₋₄₂ (12.5 μM) (B and D) peptides were
11 incubated in a fibril forming buffer in the absence (A and B) or presence of
12 ZnPc(COONa)₈ (5 μM) (C and D) for indicated time. Total fibril formed at the end
13 of incubations was evaluated by ThT fluorescence assay, as described in the
14 Materials and Methods. Data shown here are the averages ± SEM of ThT
15 fluorescence values (arbitrary unit) of at least 3 independent experiments. The
16 morphology Aβ fibrils are shown in (E). Aβ₁₋₄₀ (a and c) and Aβ₁₋₄₂ (b and d)
17 peptides (50 μM) were incubated alone (a and b) or with ZnPc(COONa)₈ (5 μM)
18 (c and d) for 72 h and 24 h, respectively. The morphology of the fibril was

1 evaluated by transmission electron microscopy as described in the Materials and
2 Methods. Bar=200 nm. (F) A β ₁₋₄₂ (100 μ M) were incubated alone or with
3 ZnPc(COONa)₈ (5 μ M) for 24 h. Aliquots of the samples were used for ThT
4 fluorescence assay (left bar). From the rest of the samples, fibrils were removed
5 by filtration and protein in the filtrates (right bar) was measured by an UV/Vis
6 spectrophotometer at 280 nm, as described in the Materials and Methods. The
7 data presented here as average \pm SEM of 3 independent experiments, and
8 expressed as percent of A β ₁₋₄₂ peptide alone (control) condition.

9 **Figure 3. Effects of ZnPc(COONa)₈ on A β fibril destabilization.** To prepare
10 fibrils, A β ₁₋₄₀ (50 μ M) and A β ₁₋₄₂ (25 μ M) peptides were incubated in a fibril
11 forming buffer for 48 h and 24 h, respectively. Indicated concentrations of
12 ZnPc(COONa)₈ were added to A β ₁₋₄₀ and A β ₁₋₄₂ fibrils resulting the final
13 concentration of the peptide were 25 μ M and 12.5 μ M, respectively, and further
14 incubated for 24 h. Total fibrils of A β ₁₋₄₀ (A) and A β ₁₋₄₂ (B) was evaluated by ThT
15 fluorescence assay. The data are the averages \pm SEM of ThT fluorescence
16 values (arbitrary unit) of at least 3 experiments. (C and D) A β ₁₋₄₀ or A β ₁₋₄₂ was
17 incubated for 48 and 24 h, respectively. Then indicated concentrations of
18 ZnPc(COONa)₈ were added to the fibril, which result the concentration of the

1 peptide reduced to 25 μ M. Two micrograms of peptide fibrils were separated
2 using 4-20% gradient Tris-Glycine SDS-PAGE, and the peptide bands of $A\beta_{1-40}$
3 (C) and $A\beta_{1-42}$ (D) species were visualized by Coomassie brilliant blue staining,
4 as described in the Materials and Methods. * $p < 0.05$, ‡ $p < 0.01$ and † $p < 0.001$ vs
5 corresponding $ZnPc(COONa)_8$ 0 μ M condition.

6 **Figure 4. Effect of Sodium Azide (NaN_3) on $ZnPc(COONa)_8$ mediated**
7 **inhibition of $A\beta$ fibril formation.** Indicated concentration of NaN_3 was added to
8 $A\beta_{1-40}$ (50 μ M) (A) and $A\beta_{1-42}$ (12.5 μ M) (B) and incubated for 48 h and 24 h,
9 respectively. To evaluate the effects of NaN_3 on $ZnPc(COONa)_8$ mediated
10 inhibition of $A\beta_{1-40}$, and $A\beta_{1-42}$ fibril formation, indicated concentrations of NaN_3
11 were added to $A\beta_{1-40}$ (50 μ M) (C) and $A\beta_{1-42}$ (12.5 μ M) (D) in the presence of
12 $ZnPc(COONa)_8$ (5 μ M), and incubated for 48 h and 24 h, respectively. The
13 amount of fibril formed after incubation was evaluated by ThT fluorescence
14 assay. Data showed here are the average \pm SEM of at least 3 experiments, and
15 presented as percent of $A\beta$ peptide alone (control) condition.

16 **Figure 5. Binding of $ZnPc(COONa)_8$ to $A\beta_{1-42}$ and change in the**
17 **hydrophobicity of the fibril forming microenvironment.** (A) $A\beta_{1-42}$ monomer
18 (50 μ M) was incubated in a fibril forming buffer with indicated concentrations of

1 ZnPc(COONa)₈ for 24 h. To evaluate the binding ability to the preformed fibril,
2 Aβ₁₋₄₂ fibril was prepared by incubating the monomer in fibril forming buffer for 24
3 h, then indicated concentration of ZnPc(COONa)₈ was added to the fibril to
4 make its final concentration 50 μM, and further incubated for 24 h. After
5 incubation, 5 μg of peptide fibrils were used for immunoprecipitation with a
6 monoclonal anti-Aβ IgG. For negative controls, normal mouse IgG, was used
7 instead of anti-Aβ IgG, or buffer containing ZnPc(COONa)₈-only was used
8 instead of Aβ₁₋₄₂. (B-D) To evaluate the hydrophobic microenvironment, Aβ₁₋₄₂
9 (12.5 μM) was incubated in the absence or presence of ZnPc(COONa)₈ (5 μM)
10 for indicated time, and ANS fluorescence assay was done, as described in the
11 Materials and Methods. Representative ANS fluorescence emission spectra of
12 Aβ₁₋₄₂ in the absence or presence of ZnPc(COONa)₈ of indicated time are shown
13 in (B). The average values of ANS fluorescence intensities (arbitrary unit) and
14 the positions of fluorescence emission maxima (nm) are shown in (C) and (D),
15 respectively. *p<0.05 and †p<0.01 vs corresponding 0 h condition; #p<0.05 and
16 ‡p<0.01 vs Aβ₁₋₄₂ condition of same time point.

17 **Figure 6. Effects of ZnPc(COONa)₈ on the secondary structures and the**
18 **oligomerization of Aβ peptide.** Aβ₁₋₄₀ (100 μM) was incubated in a fibril forming

1 buffer in the absence or presence of ZnPc(COONa)₈ (2 μM) for indicated time.
2 The samples were then diluted with H₂O to make Aβ₁₋₄₀ and ZnPc(COONa)₈
3 concentrations to 10 and 0.2 μM, respectively, and the changes in the secondary
4 structures were evaluated by CD spectroscopy. The percentage of different
5 secondary structures of a representative experiment is shown in (A). (B) Aβ₁₋₄₂
6 (50 μM) was incubated in a fibril forming buffer in the absence or presence of
7 ZnPc(COONa)₈ (5 μM) for indicated time. Two micrograms of peptide were
8 separated by 4-20% gradient Tris-Glycine SDS-PAGE, and the peptide bands of
9 Aβ₁₋₄₂ species were visualized by Coomassie brilliant blue staining, as described
10 in the Materials and Methods. (C) After incubation, 2 μg of peptides were spotted
11 on a nitrocellulose membrane, and Aβ₁₋₄₂ oligomers were detected by an
12 oligomer-specific antibody, as described in the Materials and Methods.

13 **Figure 7. Effects of ZnPc(COONa)₈ on the neuronal viability in the culture.**

14 A neuronal cell line (A1 cell) was cultured in DMEM medium containing 1% FBS
15 in the presence of indicated concentrations of ZnPc(COONa)₈ or Aβ₁₋₄₂ for 48 h.
16 Representative photomicrographs of A1 cells cultured with ZnPc(COONa)₈
17 (upper row) or Aβ₁₋₄₂ (lower row) are shown in (A). A1 cells were treated with
18 Aβ₁₋₄₂ (5 μM) and indicated concentrations of ZnPc(COONa)₈, and

1 representative photomicrographs after 48 h treatment are shown in (B). (C) After
2 treatment with indicated concentrations of $A\beta_{1-42}$ or $ZnPc(COONa)_8$ for 48 h, the
3 viability of A1 cells were evaluated by MTT assay. Average \pm SEM data of 3
4 experiments are shown in (C), where \square represents $ZnPc(COONa)_8$ and \blacksquare
5 represents $A\beta_{1-42}$. (D) A1 cells were cultured with $A\beta_{1-42}$ (5 μ M) and indicated
6 concentrations of $ZnPc(COONa)_8$ for 48 h, and cell viability was evaluated by
7 MTT assay, as described in the Materials and Methods. The data presented in
8 (C) and (D) as percent control, where viable cells in normal culture were
9 considered as control. * $p < 0.05$ vs $ZnPc(COONa)_8$ 0 μ M conditions.

10

Figure 1

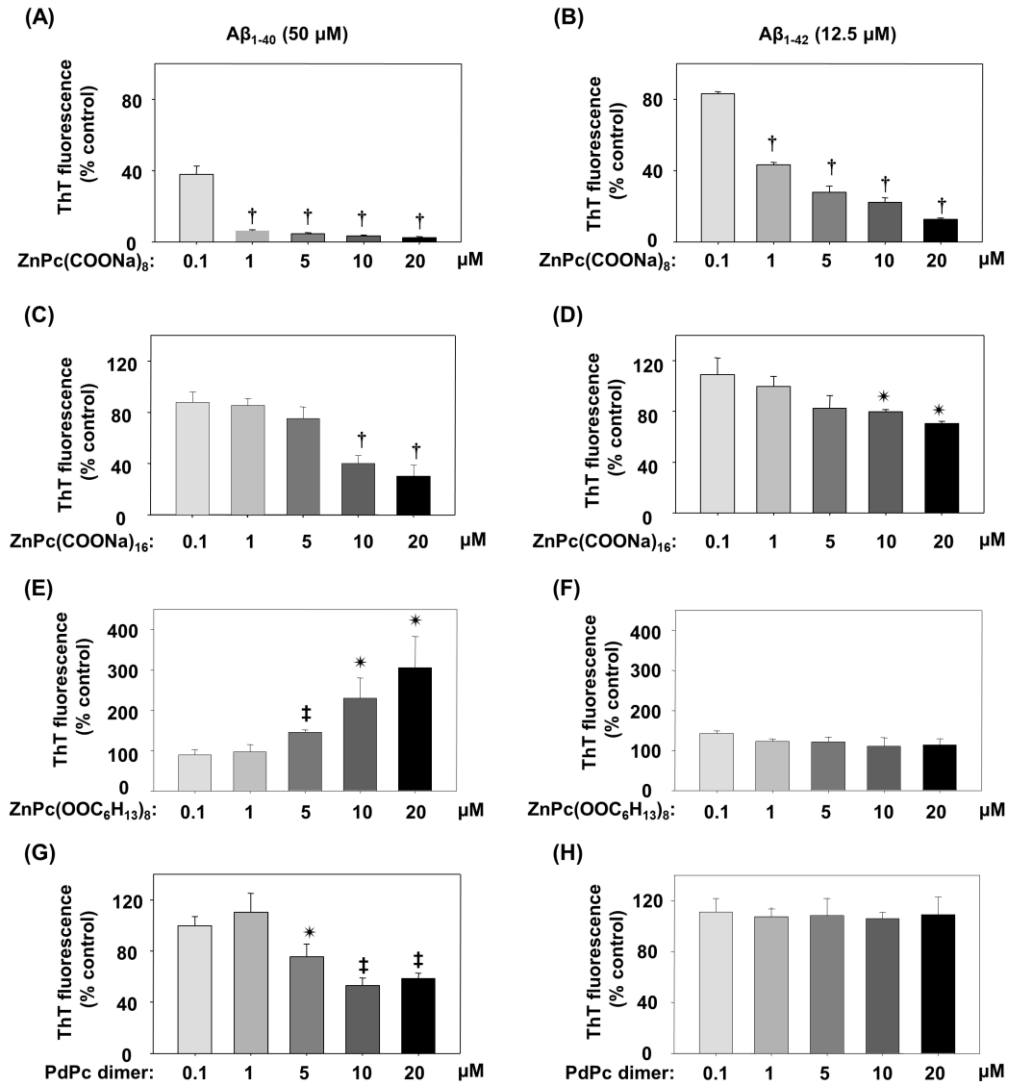


Figure 2

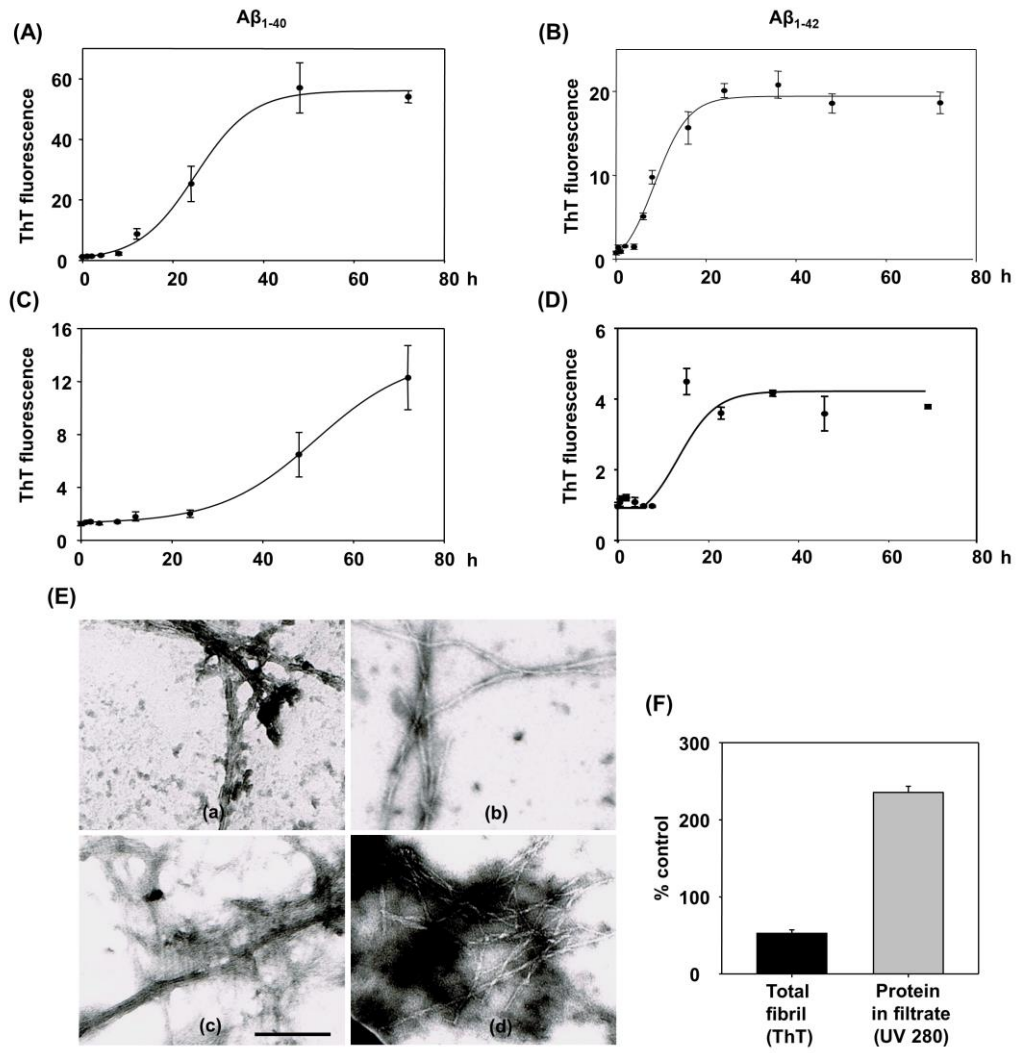


Figure 3

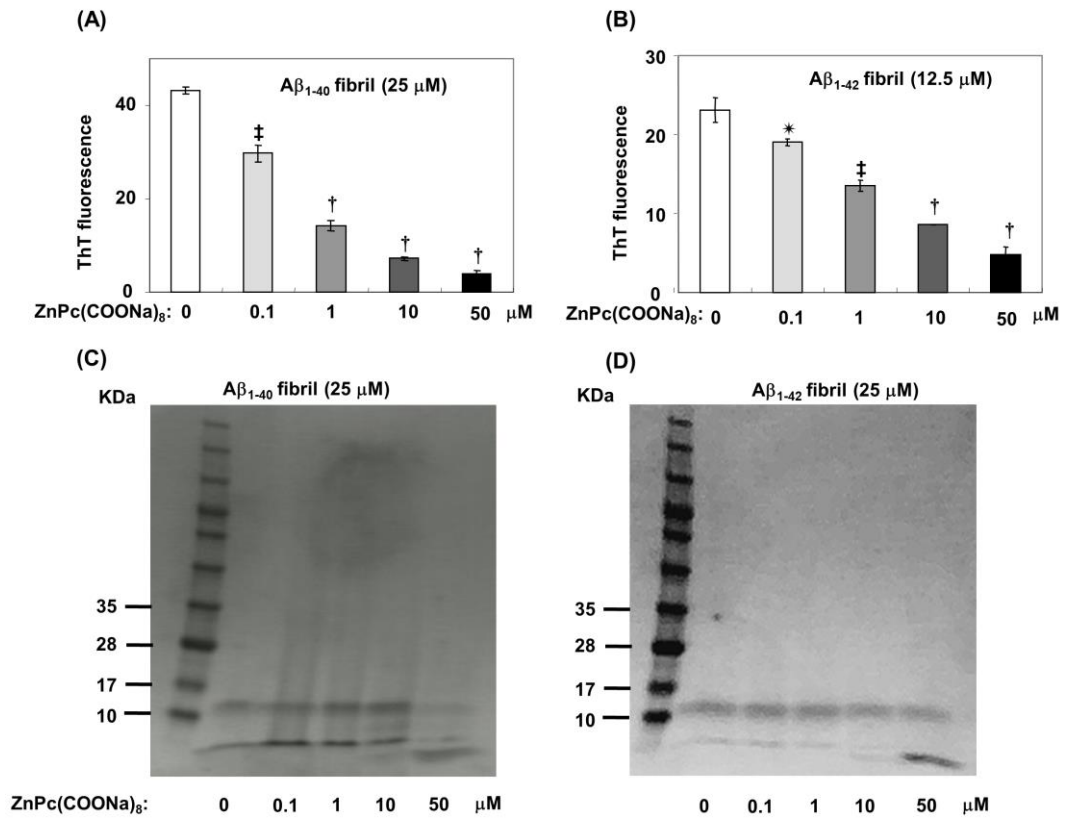


Figure 4

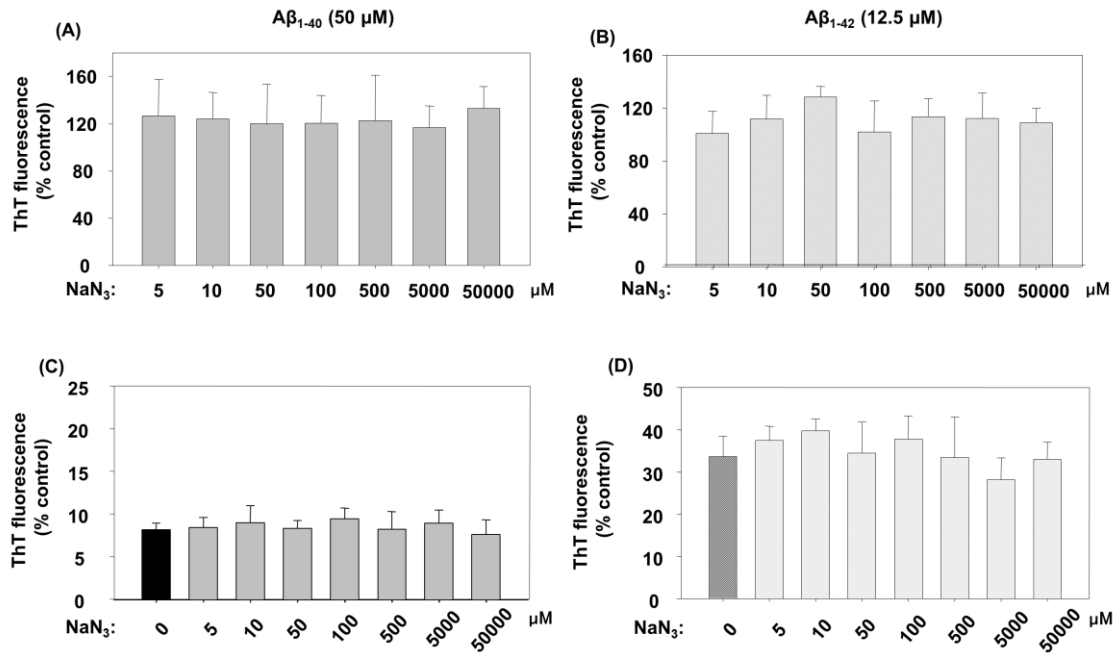


Figure 5

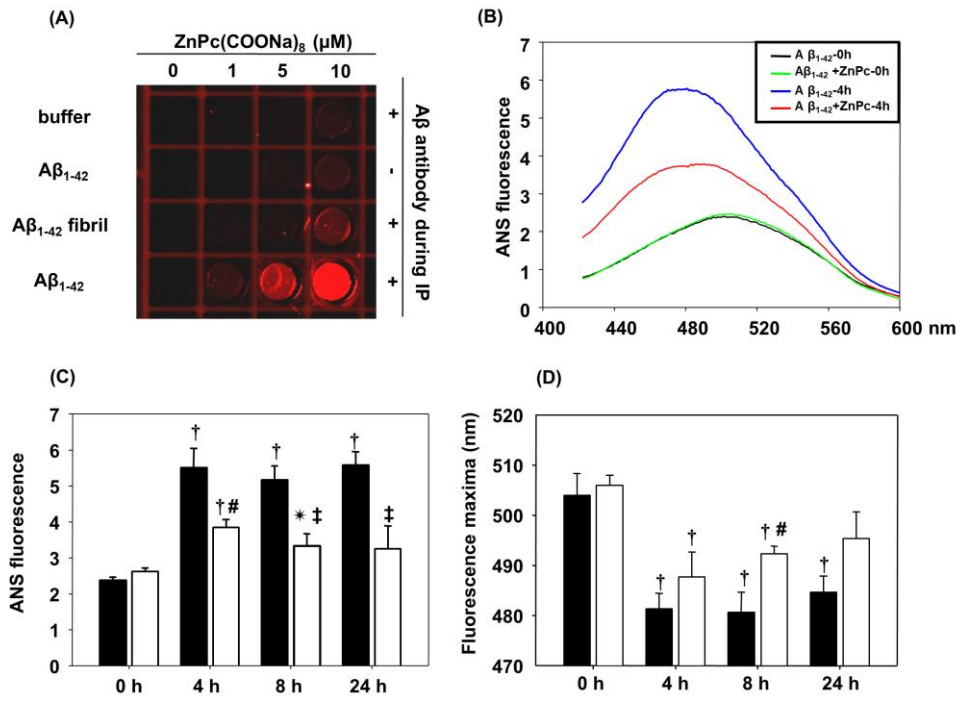


Figure 6

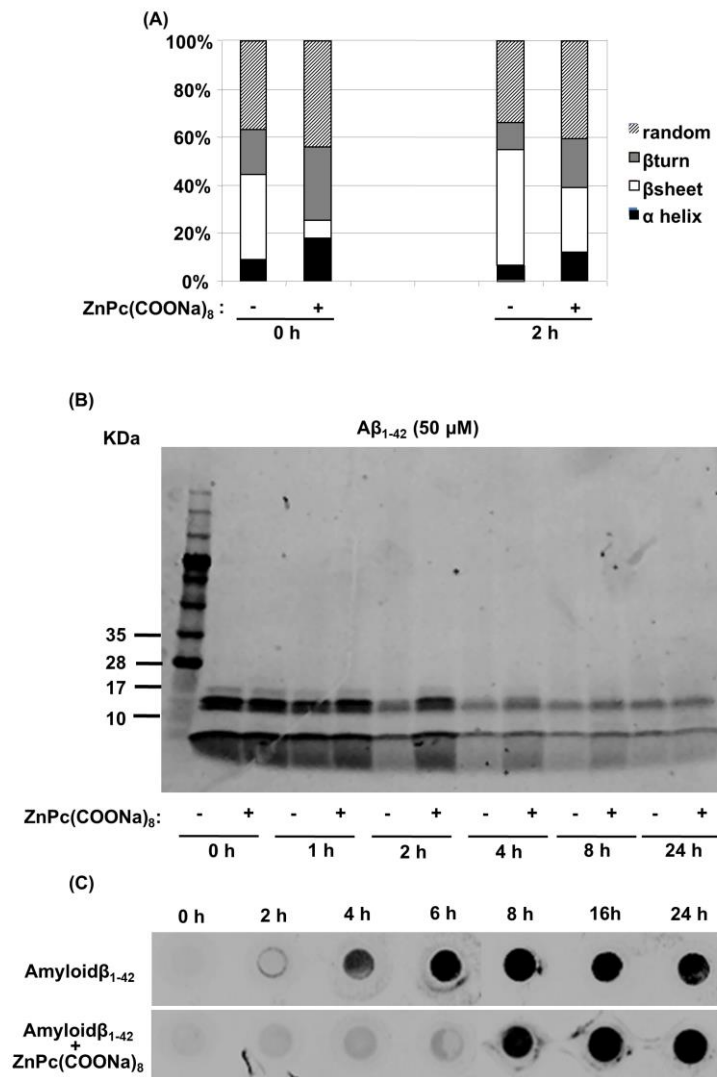


Figure 7

